

Driven Disordered Periodic Media with an Underlying Structural Phase Transition

Ankush Sengupta and Surajit Sengupta
 Satyendra Nath Bose National Centre for Basic Sciences,
 Block-VD, Sector-III, Salt Lake, Kolkata 700 098, India

Gautam I. Menon
 The Institute of Mathematical Sciences, CIT Campus, Taramani, Chennai 600 113, India
 (Dated: January 2, 2022)

We investigate the driven states of a two-dimensional crystal whose ground state can be tuned through a square-triangular transition. The depinning of such a system from a quenched random background potential occurs via a complex sequence of dynamical states, which include plastic flow states, hexatics, dynamically stabilized triangle and square phases and intermediate regimes of phase coexistence. These results are relevant to transport experiments in the mixed phase of several superconductors which exhibit such structural transitions as well as to driven colloidal systems whose interactions can be tuned via surface modifications.

PACS numbers: 74.25.Qt, 61.43.jg, 83.80.Hj, 05.65.+b

The description of phases and phase transitions in driven steady states is a central theme in the statistical mechanics of non-equilibrium systems[1]. A variety of such states are obtained in the depinning and flow of randomly pinned, periodic media, such as charge-density wave systems and Abrikosov flux-line lattices in the mixed state of type-II superconductors[2]. Many such superconductors exhibit structural transitions in the mixed state, typically between flux-line lattices with triangular and rectangular symmetry [3]. Colloidal systems such as PMMA spheres coated with a low-molecular-weight polymer undergo a remarkable variety of solid-solid transformations in an external field[4]. While applying a sufficiently large current depins the flux lines from the quenched random disorder present in all real materials, the possibility of driving colloidal particles in two dimensions across a disordered substrate has also been raised [5]. What links these diverse systems is the generic problem of understanding the competition between an underlying structural phase transition in a pure periodic system as modified by disorder, and the non-equilibrium effects of an external drive. This Letter proposes and studies a simple model which describes this physics.

Our model system is two-dimensional and consists of particles with two and three-body interactions[6]. The three-body interaction, parameterized through a single parameter v_3 , tunes the system across a square-triangular phase transition. Our central result, the sequence of steady states obtained as a function of increasing force F for various values of v_3 , is summarized in the dynamical "phase" diagram of Fig. 1. We obtain a variety of phases: pinned states which may have dominantly triangular or square correlations, a moving liquid/glass phase, a moving hexatic glassy phase, flowing triangular and square states ordered over the size of our simulation cell and a dynamic coexistence regime between these ordered phases. We discuss our characterization of these states

and the applicability of simple dynamical criteria for non-equilibrium phase transitions between them.

The model: Particles interact in two dimensions through the interaction potential $U = \frac{1}{2} \sum_{i \neq j} V_2(r_{ij}) + \frac{1}{6} \sum_{i \neq j \neq k} V_3(r_i; r_j; r_k)$, where r_i is the position vector of particle i , $r_{ij} = |r_i - r_j|$, $V_2(r_{ij}) = v_2 (\frac{r_0}{r_{ij}})^{12}$ and $V_3(r_i; r_j; r_k) = v_3 [f_{ij} \sin^2(4\theta_{ijk}) f_{jk} + \text{permutations}]$ [6]. The function $f_{ij} = f(r_{ij}) = (r_{ij} - r_0)^2$ for $r_{ij} < 1.8 r_0$ and 0 otherwise and θ_{ijk} is the angle between r_{ji} and r_{jk} . The two-body (three-body) interaction favours a triangular (square) ground state. Energy and length scales are set using $v_2 = 1$ and $r_0 = 1$. Particles also interact with a quenched random background modeled as a Gaussian random potential [7] $V_d(r)$ with zero mean and exponentially decaying (short-range) correlations, The disorder variance is set to $v_d^2 = 1$ and its spatial correlation length is $\xi = 0.12$. The system evolves through standard Langevin dynamics; $\dot{r}_i = v_i$ and $\dot{v}_i = \frac{F_i^{\text{int}}}{m} + F + \eta_i(t)$. Here v_i is the velocity, F_i^{int} the total interaction force, and $\eta_i(t)$ the random force acting on particle i . A constant force $F = F F_x / 0g$ drives the system and the zero-mean thermal noise $\eta_i(t)$ is specified by $\langle \eta_i(t) \eta_j(t^0) \rangle = 2T \delta_{ij} \delta(t - t^0)$ with $T = 0.1$, well below the equilibrium melting temperature of the system. The unit of time $\tau = \frac{r_0^2}{v_2} = 1$ with $\eta = 1$ the viscosity.

Simulation details: Our system consists of 1600 particles in a square box at number density $\rho = 1.1$. At $T = 0.1$, the pure system remains triangular upto $v_3 = 1.5$. For larger v_3 , a square phase is obtained. Larkin length estimates [2] yield $L_a \approx a/100$, with $a = 1 = r_0^2$ the lattice parameter, somewhat larger than our system size.

Equilibration in the disorder potential is achieved through a simulated annealing procedure in which the disorder potential is varied by increasing its strength from zero to unity in small steps. The system is stabi-

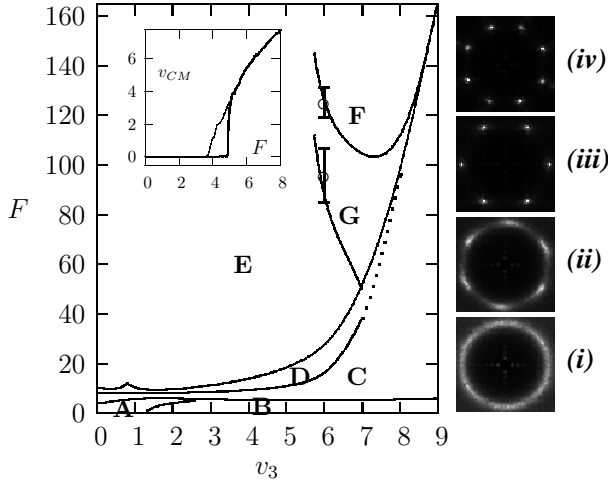


FIG. 1: The dynamical phase diagram in the v_3 - F plane. The phases are: A { pinned triangle, B { pinned square, C { plastic flow/isotropic liquid, D { moving hexatic, E { moving triangle, F { moving square and G { dynamic square-triangle coexistence. Two points with error bars show the boundary of G for $v_3 = 6$, obtained by averaging over 24 disorder realizations, as an example. The boundaries for all other transitions are considerably sharper. The inset shows the centre of mass velocity v_{cm} as a function of the driving force F as the force is increased (bold) and then decreased across the depinning transition. The right panel shows $S(q)$ for the plastic flow state (i), hexatic glass (ii), triangular solid (iii) and square solid phases (iv) at $v_3 = 6$; 0 and $F = 10$; 20; 60 and 140 respectively. To obtain $S(q)$, 50 independent configurations were used. The structure in (iv) reflects the presence of two mutually misoriented square crystallites.

lized for a minimum of 2×10^5 Monte Carlo steps at each disorder strength. Such annealed configurations are our initial inputs to the Langevin simulations. We evolve the system using a time step of 10^{-4} . The external force F is ramped up from a starting value of 0, with the system maintained at upto 10^8 steps at each F .

Observables: We monitor structural observables, such as the static structure factor $S(q) = \langle \exp(iq \cdot r_{ij}) \rangle$. Delaunay triangulations yield the probability distributions $P(n)$ of $n = 4; 5; 6$ and 7 coordinated particles ($\sum_n P(n) = 1$) [8]. We define order parameters $\phi_4 = (P(4) - P(6)) / (P(4) + P(6))$ to distinguish between square and triangular phases, $\phi_5 = (P(5) - P(7)) / (P(5) + P(7))$ to distinguish between liquid (disordered) and triangular crystals and $\phi_6 = (P(6) - P(7)) / (P(6) + P(7))$ to distinguish between liquid and square crystals. In addition, we compute the hexatic order parameter $\phi_6 = \langle \exp(i6\theta_{ij}) \rangle$ and its correlations, where θ_{ij} is the bond angle measured with respect to an arbitrary external axis. The dynamical variables we study include the center of mass velocity v_{cm} , the particle flux and its statistics and the Koshelev-Vinokur (KV) "shaking temperature" T_a [9] appropriate

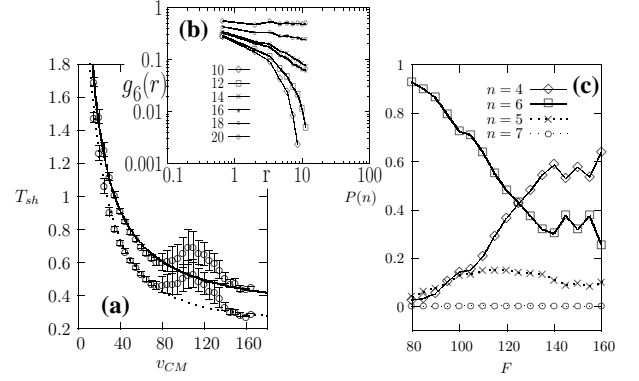


FIG. 2: (a) The shaking temperatures for a system with $v_3 = 6$ as a function of F in the drive (x) and transverse (y) directions. These are obtained by averaging over 100 independent configurations as well as over 25 separate disorder realizations. For F in the coexistence region there is a significant enhancement of the shaking temperature in excess of the prediction of KV (Ref. [9]). The lines represent fits to the KV form. (b) The hexatic correlation function $g_6(r)$ at varying force values at $v_3 = 6$, averaged over 50 independent configurations, (c) $P(n)$ for $n = 4; 5; 6; 7$ (see text) vs F averaged as in (a).

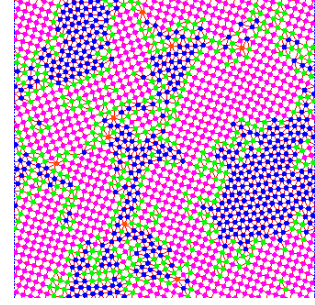


FIG. 3: (color-online) A single particle configuration showing square-triangle coexistence at $F = 107$ together with the computed Delaunay mesh. The particles are colored according to the number of neighbors $n = 4$ (magenta), 5 (green), 6 (blue) and 7 (orange). Particles with coordination 5 are present mainly in the interfacial region while those with 7 are associated with isolated dislocations.

to the drive and transverse directions and obtained from $T_s = \hbar \sqrt{v_{cm}^2} / \sum_{i=2}^{\infty} \langle \exp(i6\theta_{ij}) \rangle$, $\theta = x/y$.

For small F the solid is pinned. A disorder broadened version of the equilibrium triangle (A) to square (B) transition results as v_3 is varied across the $T = 0$ transition value at small F ; here and below alphabets in brackets refer to the states labelled in Fig. 1. The triangular (A) phase is favoured at non-zero F . Upon further increasing F , the system undergoes a discontinuous depinning transition which exhibits prominent hysteresis behaviour (Fig. 1, inset). Such a depinned state is inhomogeneous and undergoes plastic flow [10, 11, 12, 13, 14, 15] con-

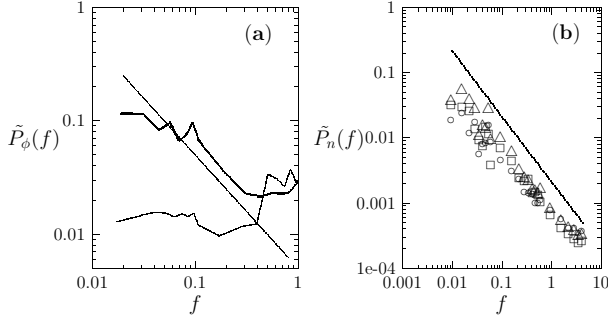


FIG. 4: (a) The power spectrum $P_\phi(f)$ of current fluctuations in the moving triangle phase (thin line $F = 55$) and in the coexistence region (bold line $F = 100$), logarithmically binned and plotted for a range of frequencies below the washboard frequency. Current fluctuations in the coexistence region are enhanced, also showing a $1=f$ decay at intermediate frequencies. (b) $P_n(f)$ for the fluctuations of the numbers of 4 (○); 5 (□) and 6 (△) coordinated particles in the coexistence region. The number of 7 coordinated particles (not shown) is vanishingly small. The straight line in both figures represents the $1=f$ law.

sistent with earlier numerical work. For larger F the velocity approaches the asymptotic behaviour $v_{CM} = F$.

The structure factor $S(q)$ of the plastically moving phase (C) obtained just above the depinning transition consists of liquid-like isotropic rings (Fig. 1(d)). Upon increasing F , the circular ring in $S(q)$ concentrates into six smeared peaks which we associate with a hexatic glass (D) [16]. Fig. 2(b) shows the evolution of the hexatic correlation function $g_6(r) = \langle h_6(0) h_6(r) \rangle$, as F is varied across (C) → (D) → (E). Note the sharp exponential decay of hexatic correlations in (C), the power-law or quasi-long-range order (QLRO) decay in (D) and the saturation (LRO) of this correlation function in regime (E). The plastic flow regime (C) expands at larger v_3 [17]. On further increasing F , the hexatic glass recrystallizes into a structure which depends on the value of v_3 : for low v_3 the nalcystal is triangular (E) whereas for large v_3 it is square (F). For intermediate v_3 the system first freezes into a triangular structure but subsequently transforms into the square via an intervening "coexistence" regime (G) best described as a mosaic of dynamically fluctuating square and triangular regions.

The phase diagram of the pure system in thermalequilibrium accommodates fluid, triangular solid and square solid phases [6]. In the driven system, as F is increased, analogous phases appear in approximately the inverse order to the sequence obtained in the pure case as T is increased. This observation agrees roughly with the KV proposal [9], which identifies the shaking temperature T_s with T . The shaking temperatures are predicted to fall as $1=v^2$ and as $1=v$ in the drive and the transverse directions respectively, consistent with our observations

in Fig. 2(a). We find that T_s is nearly independent of v_3 . Importantly, within the putative coexistence regime, T_s behaves non-monotonically, implying a breakdown of the KV prediction (see Fig. 2(a)). Typically, for a particular disorder configuration and for $5.5 < v_3 < 8.5$, T_s appears to increase sharply at a well defined F , signifying the start of coexistence. Within G, T_s remains high but drops sharply at the upper limit of G, to continue to follow the interrupted KV behavior. The limits of the coexistence region, though sharp for any typical disorder realization, vary considerably between realizations.

Within the coexistence region the probability of obtaining triangular (square) regions appears to decrease (increase) roughly linearly with F ; see Fig. 2(c). Real space configurations (Fig. 3) exhibit islands of square and triangular coordination connected by interfacial regions with predominantly 5 coordinated particles. Particles with coordination 7 are typically associated with dislocations which are scattered randomly in the interface. This configuration, in the co-moving frame, is extremely dynamic, with the islands rapidly interconverting between square and triangle. This interconversion has complex temporal properties: the power spectrum of coordination number fluctuations shows a prominent $1=f$ fall off over several decades. In addition, particle current fluctuations are enhanced by an order of magnitude, also displaying a regime of $1=f$ behavior (Fig. 4), although over a restricted range as a consequence of the proximity to the washboard frequency. This result would be hard to interpret in the absence of a genuine coexistence phase: above the depinning transition, increasing the driving force would naively be expected to reduce current noise monotonically, as observed in all previous simulation work on related models [12, 13, 14].

Renormalization group arguments suggest that neither translational LRO nor QLRO survive in the disordered moving state in two dimensions at any finite drive [18, 19, 20], their closest analog being the moving Bragg glass state argued to be stable in three dimensions and higher [20]. The ordered square (F) and triangular (E) states we obtain at large drives are then to be understood as a finite size effect arising from the restricted size of our simulation box, although the crossover length scales can be very large at weak disorder [18, 20]. The possibility of alternative dynamically stabilized states with reduced levels of ordering, such as driven transverse smectics, is attractive [18, 21]. In contrast to some previous work [11, 13, 14], we see no evidence for smectic order and flow in weakly coupled channels at large drives (our channels always remain strongly coupled (but note that moving states in which channels transverse to the drive direction are effectively decoupled may be stabilized at higher levels of thermal noise or randomness [4]).

No general arguments seem to rule out QLRO in the "moving hexatic glass" phase in two dimensions and our simulations support this possibility; see also Ref. [16].

The drive-induced stabilization of the triangular lattice state we obtain, even well into regimes where v_3 would favour a square, is an unusual result. Our finding of a distinct coexistence regime (G) separate from plastic flow states, hexatic and crystal, is novel. Such coexistence occurs in a narrow and reproducible regime in parameter space and is characterized by a variety of dynamic anomalies, including enhanced noise signals with $1/f$ character. The coexistence state appears to be a genuine non-equilibrium state, separated from other regimes through sharp non-equilibrium transitions.

Theoretical work has, so far, neglected the possibility of such dynamic phase coexistence in the non-equilibrium steady states of driven disordered crystals[21]. A non-disordered but frustrated system closely related to the one considered here has been proposed recently as a model for the dynamic heterogeneity seen in the glassy state[22]. In this model, fluctuating regions of crystalline ordering within a liquid background are argued to be responsible for the anomalous dynamic behaviour and slow relaxation in the glassy state, a physical picture which shares some similarities to our ideas regarding the coexistence regime.

In conclusion, we have shown here that the competition between structural phase transitions in a pure system as modified by disorder, coupled to the non-equilibrium effects of an external drive, can have a variety of non-trivial consequences. The ubiquity of structural phase transitions in the vortex state of a large number of superconductors which have been studied recently, as well as the relative ease with which the vortex state can be driven, suggests experimental situations in which the ideas here should find application. Functionalized colloidal particles driven over random substrates constitute a novel system on which our proposals can be tested [5, 23]. Such systems have the further advantage that interparticle interactions can be tuned both through surface modifications and through the application of external fields[23].

The authors thank M. Rao, J. Bhattacharya and A. Chaudhuri for discussions. This work was partially supported by the DST (India).

[1] Special Section on Nonequilibrium Statistical Systems, M. Barmalier, *Current Science* 77 (3), 402 (1999).

[2] T. Giamarchi and S. Bhattacharya, in *High Magnetic*

Fields: Applications in Condensed Matter Physics and Spectroscopy, ed. C. Berthier et al., Springer-Verlag, (2002), p 314.

- [3] C.D. Dewhurst, S.J. Levett, and D.M. C.K. Paul, *Phys. Rev. B* 72, 014542 (2005); L.Ya. Vinnikov et al, *Phys. Rev. B* 64, 220508(R) (2001); B. Rosenstein et al, *Phys. Rev. B* 72, 144512 (2005); S.P. Brown et al, *Phys. Rev. Lett.* 92, 067004 (2004); R. Gilardi et al, *Phys. Rev. Lett.* 93, 217001 (2004)
- [4] A. Yethiraj and A. van Blaaderen, *Nature* 421, 513 (2003); A. Yethiraj et al, *Phys. Rev. Lett.* 92, 058301 (2004)
- [5] A. Pertsinidis and X.S. Ling, *Bull. Am. Phys. Soc.* 46, 181 (2001); *ibid*, 47, 440 (2002); C. Reichhardt and C.J. Olson, *Phys. Rev. Lett.*, 89, 078301, (2002).
- [6] M. Rao and S. Sengupta, *J. Phys: Condens. Mat.* 16, 7733 (2004), *Phys. Rev. Lett.* 91, 045502 (2003);
- [7] E.M. Chudnovsky and R.D. Ickmann, *Phys. Rev. B*, 57, 2724, (1998); A. Sengupta, S. Sengupta and G.J. Memon, *Europhys. Lett.*, 70, 635 (2005).
- [8] F.R. Pappas and M.I. Sham, *Computational Geometry: An Introduction*, Springer-Verlag, New York (1985)
- [9] A.E. Koshelev and V.M. Vinokur, *Phys. Rev. Lett.* 73, 3580 (1994); S. Scheidl and V.M. Vinokur, *Phys. Rev. B* 57, 13800, (1998).
- [10] H.J. Jensen, A. Brass and A.J. Berlinsky, *Phys. Rev. Lett.* 60, 1676 (1988)
- [11] K. Moon, R.T. Scalettar and G.T. Zimanyi, *Phys. Rev. Lett.* 77, 2778 (1996)
- [12] M.C. Faleski, M.C. Marchetti and A.A. Middleton, *Phys. Rev. B* 54, 12427 (1996)
- [13] C.J. Olson, C. Reichhardt and F. Nori, *Phys. Rev. Lett.* 81, 3757, (1998).
- [14] H. Fangohr, S.J. Cox and P.A.J. de Groot *Phys. Rev. B*, 64, 064505, (2001)
- [15] M. Chandran, R.T. Scalettar and G.T. Zimanyi, *Phys. Rev. B* 67, 052507 (2003)
- [16] S. Ryu, A. Kapitulnik, and S. Doniach, *Phys. Rev. Lett.* 77, 2300 (1996).
- [17] Although the plastic flow regime expands as v_3 is increased over the scales shown in Fig. 1, it collapses at much larger $v_3 \sim 30$ (not shown).
- [18] L. Balents, M.C. Marchetti and L. Radzihovsky, *Phys. Rev. Lett.* 78, 751 (1997); *Phys. Rev. B* 57, 7705 (1998).
- [19] S. Scheidl and V.M. Vinokur, *Phys. Rev. E* 57, 2574, (1998).
- [20] P. Ledoussal and T. Giamarchi, *Phys. Rev. B* 57, 11356 (1998).
- [21] T. Nattermann and S. Scheidl, *Adv. in Phys.* 49, 607 (2000).
- [22] H. Shintani and H. Tanaka, *Nature Physics* 2 200 (2006)
- [23] A. van Blaaderen, *Nature*, 439, 545, (2006).